Consolidation and atmospheric drying of fine oil sand tailings
Comparison of blind simulations and field scale results

Vardon, Phil; Yao, Yutian; van Paassen, Leon; van Tol, Frits

Publication date
2016

Document Version
Accepted author manuscript

Published in
Proceedings of IOSTC2016

Citation (APA)
Vardon, P., Yao, Y., van Paassen, L., & van Tol, F. (2016). Consolidation and atmospheric drying of fine oil sand tailings: Comparison of blind simulations and field scale results. In D. C. Sego, G. W. Wilson, & N. A. Beier (Eds.), *Proceedings of IOSTC2016: Lake Louise, USA* (pp. 396-407). University of Alberta.

CONSOLIDATION AND ATMOSPHERIC DRYING OF FINE OIL SAND TAILINGS: COMPARISON OF BLIND SIMULATIONS AND FIELD SCALE RESULTS

Philip J. Vardon[1], Yutian Yao[1], L.A. van Paassen[1] and A. Frits van Tol[1,2]
[1]Delft University of Technology, Delft, the Netherlands
[2]Deltares, Delft, the Netherlands

ABSTRACT

This paper presents a comparison between blind predictions of field tests of atmospheric drying of mature fine tailings (MFT) presented in IOSTC 2014 and field results. The numerical simulation of the consolidation and atmospheric drying of self-weight consolidating fine material is challenging and requires significant knowledge of the material, climate and the interaction between the two. This paper presents the outcome of a study which developed a numerical model, undertook material characterization and predicted the behaviour of full scale field tests undertaken in Shell Canada's Muskeg River Mine near Fort McMurray, Alberta. The blind predictions were published in IOSTC 2014. A comparison between the observed and simulated behaviour in terms of settlement and void ratio yields a number of conclusions regarding the model: (i) all of the major observed features can be predicted by the numerical model; (ii) the quantification of the behaviour is well represented; (iii) due to the fast initial consolidation, the amount of material recorded as being deposited was underestimated; (iv) significant shear strength development requires a void ratio reduction which either requires a significant overburden or atmospheric drying.

INTRODUCTION

Mature fine tailings (MFT) are the fine tailings that arise from initial disposal of the tailings in settling ponds, where the dense solids with a large particle size (i.e. sands) settle to the bottom, water without solids remains at the top and can be recycled. The remaining middle layer is composed of the fine particles and a high water content, known as MFT. These tailings suffer from high volume, extremely low shear strength and extremely long settling times.

A number of techniques have been developed to deal with such tailings, one of which is flocculation, via addition of a chemical flocculent, and atmospheric drying in layers. Shell Canada have investigated this possibility resulting in a proposed flocculent and a series of field scale tests at the Muskeg River Mine near Fort McMurray, Alberta. Delft University of Technology has supported this work via an experimental and numerical project, with a summary of the experimental work presented in this conference (Yao et al., 2016) and previously (Yao et al., 2012, 2014). The numerical model was originally presented by van der Meulen et al. (2012) and further developed and validated by Vardon et al. (2014), including blind predictions of the behaviour of the field tests. Some further theoretical analyses were undertaken looking at the most efficient method of layering, to yield the most reduction in volume and even density (Vardon et al., 2015).

This paper presents the results of a comparison between the blind predictions presented by Vardon et al. (2014) and the results of the field tests. Additional simulations were undertaken where deviations were found to investigate the causes of the deviations. The numerical model and the field tests are initially briefly outlined as background to the results.

NUMERICAL MODEL

Governing equations

While consolidation is typically, and generally, solved using two coupled equations (e.g. Biot 1941), the self-weight consolidation of deposited liquid material is mostly driven by shrinkage and is typically stored in deposits which are much wider than deep and therefore can be considered 1D. Therefore, in this work, a 1D model where the hydraulic behaviour is primarily solved is appropriate. The deformation is then calculated in a second step, based on the results of the hydraulic model.

The governing equation is therefore based upon the conservation of water mass and utilizes

Darcy's Law to calculate the water flow. The water potential includes the following components:

- Elevation
- Overburden
- Suction/pressure.

The equation solved (after Kim et al., 1992) is:

$$\frac{\partial \Theta}{\partial \mathrm{t}} = \frac{\partial}{\partial z}\left[K\frac{\partial}{\partial z}(\varphi + z + \Omega)\right] \qquad (1)$$

where Θ is the volumetric water content (V_w/V_t), t is time, z is the elevation, K is the hydraulic conductivity, φ is the water potential, i.e. the suction or the pressure, and Ω is the overburden component.
By expanding the spatial differential of the water potential, i.e. the part inside the square bracket of eq. (1) and ignoring any surcharge, yields:

$$\frac{\partial \Theta}{\partial \mathrm{t}} = \frac{\partial}{\partial z}\left[K\left(\begin{array}{c}\frac{\partial \varphi}{\partial \theta}\cdot\frac{\partial \theta}{\partial z} + 1 + \\ \gamma\frac{\partial e}{\partial \theta} + \frac{\partial^2 e}{\partial \theta^2}\int_{z_0}^{z}\gamma\,\mathrm{d}z\cdot\frac{\partial \theta}{\partial z}\end{array}\right)\right] \qquad (2)$$

where θ is the water ratio (V_w/V_s), e is the void ratio (V_v/V_s) and γ is the volumetric weight of the material. The water content is related to the water ratio as $\Theta = \theta/(1+e)$.

Two sets of coordinates have been defined: Cartesian coordinates, where z is the vertical coordinate in real space, and Lagrangian coordinates, where the same solid material always has the same position, and m is the vertical coordinate, defined as $\mathrm{d}m = \mathrm{d}z/(1+\mathrm{e})$. This is useful to understand how the material evolves.

At each position in the soil column and in time $\partial\varphi/\partial\theta$ can be calculated from the Soil Water Retention Curve, and $\partial \mathrm{e}/\partial\theta$ and $\partial^2 e/\partial\theta^2$ can be calculated from the shrinkage curve. K changes as the void ratio changes, so must also be updated.

Boundary conditions

To simulate both consolidation behaviour and evaporation (and precipitation) a competitive boundary condition has been incorporated at the top surface.

Potential evaporation, rainfall, permeability restricted flow and consolidation driven flow are all calculated and the dominant mechanism used as a flux boundary condition.

FIELD TESTS

Three field tests were undertaken, the first termed the '*Deep stack*', where only a single layer was deposited, the second termed '*Thick multi-lift*' where three thick layers (lifts) were deposited and the third termed '*Thin multi-lift*' where seven thin layers were deposited. Approximately the same amount of material was deposited in each test. Table 1 gives the layer thicknesses for each test and layer.

Table 1. Field test layer thicknesses for the three field tests.

Test	Lift	Days from start	Reported layer thicknesses (cm)	Post-analysis layer thicknesses (cm)
Deep stack	1	0	450.0	480.0
Thick multi-lift	1	0	100.0	130.0
	2	257	180.0	230.0
	3	346	130.0	150.0
Thin multi-lift	1	0	90.0	100.0
	2	37	50.0	80.0
	3	257	50.0	60.0
	4	290	50.0	50.0
	5	317	60.0	60.0
	6	346	110.0	130.0
	7	365	40.0	50.0

RESULTS

The analyses were undertaken with the material parameters as reported in Vardon et al. (2014), determined based upon the experimental work presented in Yao et al. (2012, 2014).

The atmospheric drying is the critical forcing parameter, so has been reproduced here in Figure 1. Via an initial sensitivity analysis it was found that averaging the precipitation and evaporation potential monthly gave good results and allowed the numerical model to run efficiently. The model run time was between 30 secs and 5 minutes, and was variable on the non-linearity of the fluxes and the steepness of the gradients in the system.

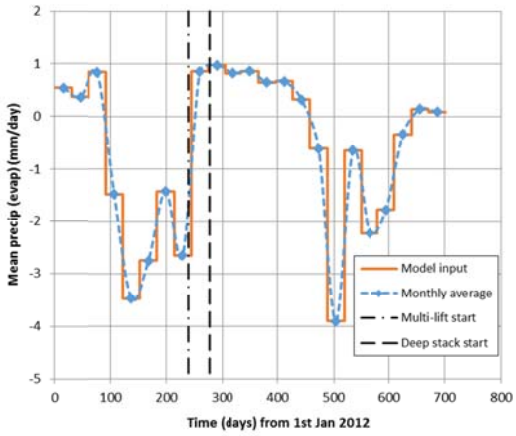

Figure 1. Mean precipitation averaged per month. Negative mean precipitation is equal to evaporation potential.

Initial results

The initial results of the Deep Stack simulation are presented in Figure 2. The solid squares are the experimental results and the blue lines the numerical simulations. In Figure 2(a) the depth is shown, with the series of blue lines every 40cm initially (shown in Figure 17 of Vardon et al., 2014). The gaps in experimental data are due to snow cover where the surface could not be observed. The results show excellent agreement with the trend of displacement, in particular at the start and where the gradients change due to evaporation, e.g. between 260 and 300 days, with an 8% underestimation of final depth.

The void ratio profiles are presented in Figure 2(b), with the time series progressing from the right of the figure to the left. The experimental profile at 374 days is overlain the results. In comparison the final numerical situation is the most left dotted red line. In general, excellent agreement between the experimental and numerical prediction was found. A dense crust is shown in both the experimental and numerical results starting from approximately 2m above the base until the surface. The numerical results show a slight overestimation of the void ratio at the base of the stack.

It is also useful to present the results in terms of material level coordinates, i.e. the same solid material always has the same coordinate, as this allows an understanding of the history of the material. This is also how the results were presented in Vardon et al. (2014). However, when this was undertaken, shown in Figure 3 (numerical results from Figure 15, Vardon et al., 2014), it was clear that there was more solid material recorded in the experiments than in the numerical model, by approximately 7%. It is hypothesized that this was the cause for the underestimation of the final stack depth. It is also thought likely as the very sharp gradient in the early part of the experiment would make the amount of material deposited very difficult to control. This same trend was observed in the *Thick multi-lift* and the *Thin multi-lift*, but increasing with each lift. These results are shown in Appendix I.

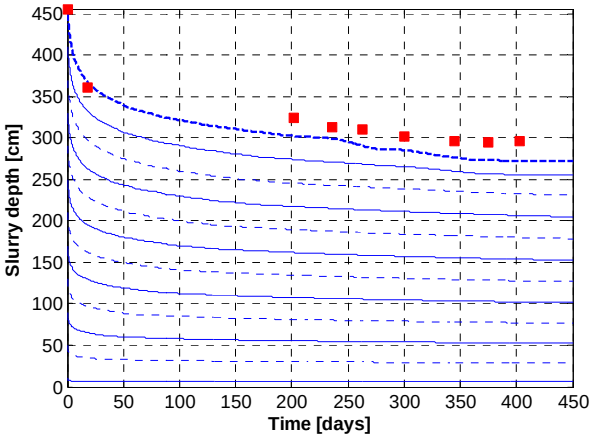

(a) Temporal evolution of the depth.

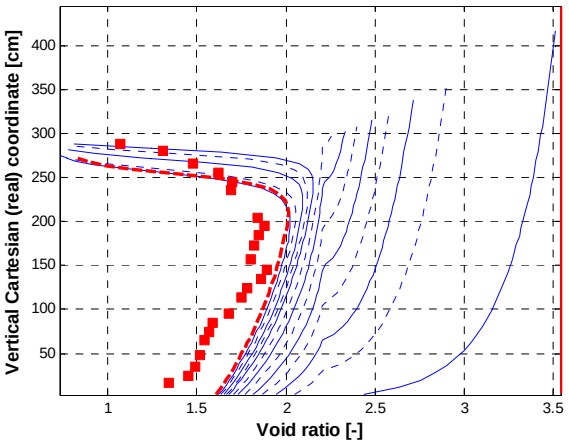

(b) Void ratio profiles, with 374 day experimental profile (squares). Final numerical result (thick dotted line) is 450 days.

Figure 2. Comparison of the results of the *Deep stack* numerical simulation against the experimental results.

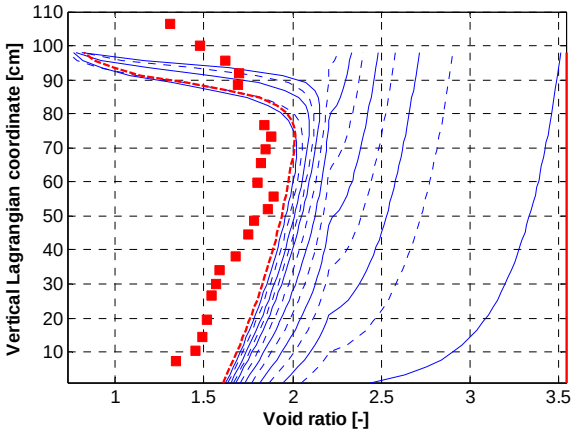

Figure 3. Comparison of the results of the *Deep stack* numerical simulation against the experimental results in material level (Lagrangian) coordinates.

Updated results with additional material

Following the conclusions that in general the trends and material behaviour seemed to be well represented, but that there was additional material deposited, a series of additional simulations were undertaken.

The simulations were identical (material parameters and boundary conditions) with the exception of addition material. The amount of additional material was calculated from the void ratio measurements, as the layering was clear (e.g. see Figure A1(b)). The updated layer thicknesses are shown in the last column of Table 1.

The results are presented below. In Figure 4 for the *Deep Stack*, in Figures 5 and 6 for the *Thick multi-stack* and in Figure 7 for the *Thin multi-stack.*

In Figure 4(a), it is seen that the additional material only affects slightly the match of the results initially, and it matches excellently later in the analysis. In Figure 4(b) the void ratio matches well in the entire thickness of the stack, although there is a slight underestimation of the reduction of void ratio at the base of the stack until the evaporative 'crust'.

In Figure 5 substantial qualitative and quantitative agreement are observed. In particular, the overall depth reduction is well matched in each layer, the void ratio is well represented throughout. Note that in the top layer the final numerical results are late than the experimentally recorded result, and the switch between consolidation and evaporative behaviour is well represented.

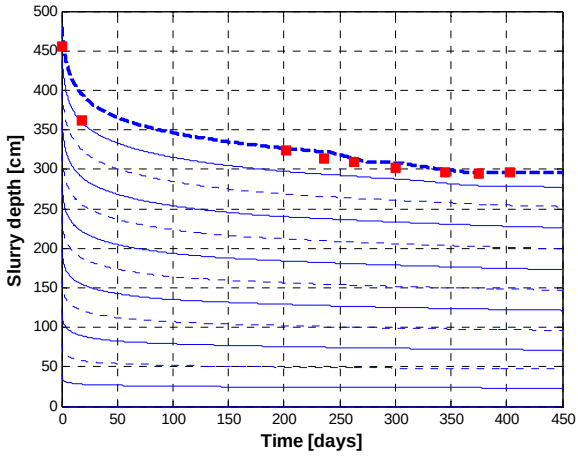

(a) Temporal evolution of the depth.

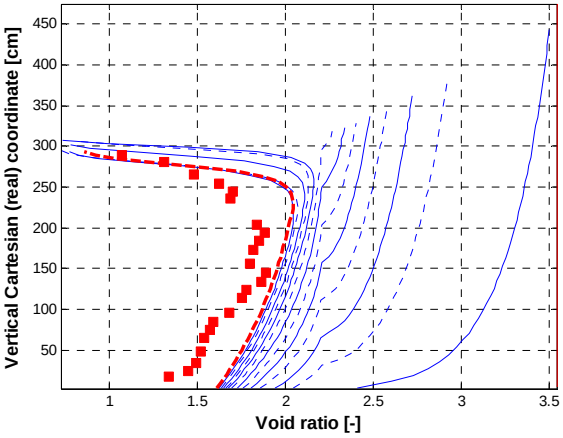

(b) Void ratio profiles, with 374 day experimental profile (squares). Final numerical result (thick dotted line) is 450 days.

Figure 4. Comparison of the results of the *Deep stack* updated numerical simulation against the experimental results.

It is noticed that the void ratio at the top of the top of the second layer is under-predicted. It is hypothesized that the reason for this difference is that this crust starts to develop just at the end of the period where the second layer is exposed to the atmosphere, due to elevated evaporative fluxes and reduced consolidation fluxes. During this time, there is a competition between the evaporative and consolidation boundary condition and the model is then sensitive to small changes in these values. This is shown in Figure 6, where the water fluxes are shown. The black box highlights the time where the crust in the second layer is

formed. The consolidation flux (the smoothly decreasing line) and the evaporative fluxes (the steady line) in this period are almost equal and therefore the crust formation is sensitive to these changes.

To increase the depth of the crust and take advantage of the evaporative behaviour, the deposition could be delayed (e.g. as suggested by Vardon et al., 2015).

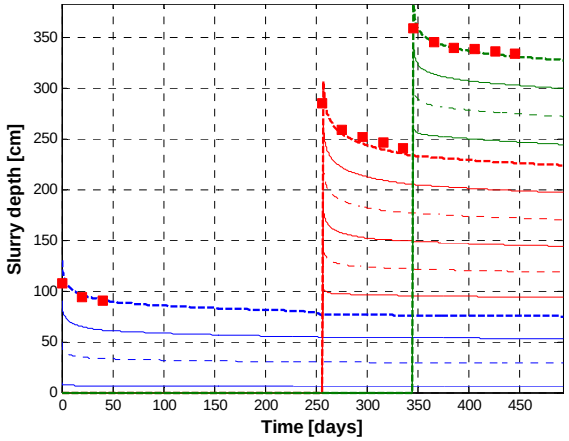

(a) Temporal evolution of the depth.

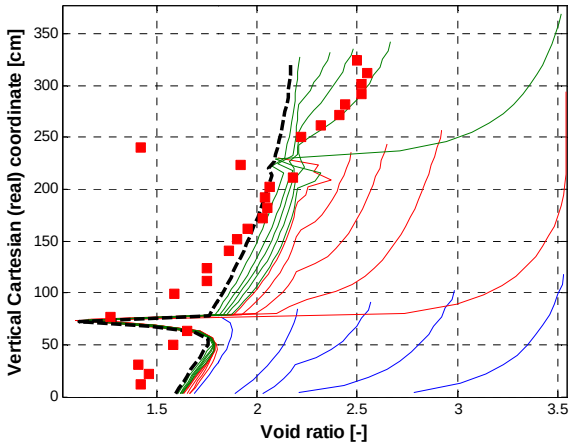

(b) Void ratio profiles, with 412 day experimental profile (squares). Final numerical result (thick dotted line) is 450 days.

Figure 5. Comparison of the results of the *Thick multi-stack* updated numerical simulation against the experimental results.

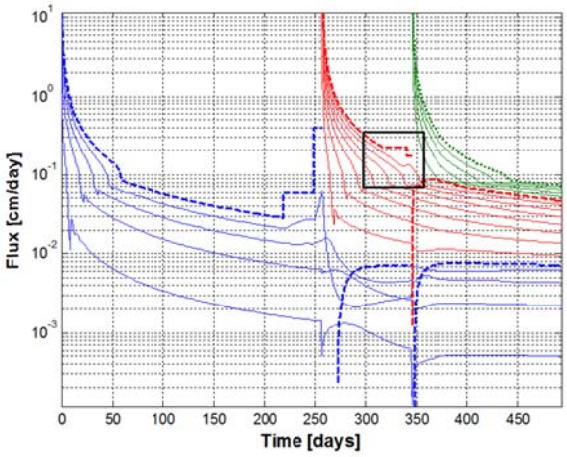

Figure 6. Water flux evolution for the *Thick multi-stack.*

In Figure 7, again substantial qualitative and quantitative agreement are observed, however there are more differences than in the prior two simulations.

The overall depth reduction is well matched, the void ratio is well represented, in particular, quantitatively in the lowest three layers and qualitatively in the upper four and the switch between consolidation and evaporative behaviour is well represented. The main differences which can be observed are that in the later stages there is some overestimation of height reduction and there is overestimation of reduction in void ratio in the upper layers.

In this test, mostly a new layer was added when the soil was still significantly consolidating, with the exception of the second layer, where the void ratio results match well the experimental results. It is hypothesised that this makes the model sensitive to variations in initial water content, the deposition process, averaging of climatic data and the behaviour of the material in very wet conditions, where settling of particles may occur (as opposed to consolidation behaviour).

RESULTS DISCUSISION

In general, the qualitative and quantitative predictions of the numerical model are in close agreement with the experimental results.

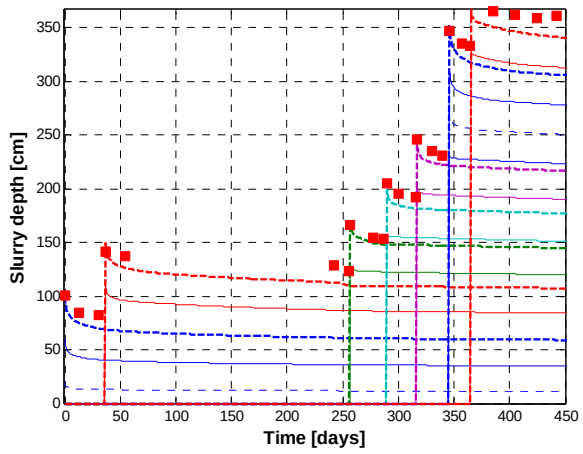

(a) Temporal evolution of the depth.

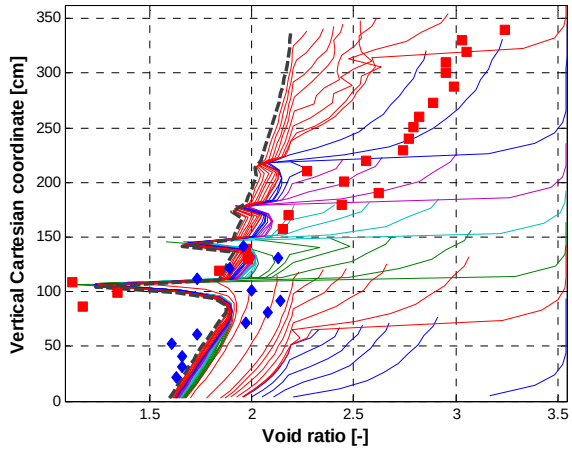

(b) Void ratio profiles, with 276 day experimental profile (diamonds) and 412 day experimental profile (squares). Final numerical result (thick dotted line) is 450 days.

Figure 7. Comparison of the results of the *Thin multi-stack* updated numerical simulation against the experimental results.

In particular, it can be seen that:

- The general settlement rates and amounts are in good agreement.
- The rates of settlement in time are very closely matching. Specifically, both the typical consolidation curve at the beginning of each layer, and the times where high evaporation are expected, are well represented.
- The void ratio (therefore material density) distribution is well predicted. Both the general trend of denser material at the base and the denser layers due to evaporation are well predicted.

It was expected to have deviation of the results from the experiments in the periods where significant snow cover was seen. However, based on the settlement gradients, while some evidence is apparent, significant deviation is not seen. Possible reasons include: limited frost depth due to the isolating snow cover, or excess pore pressures building up near the surface which can quickly dissipate when ice and snow melts or warmer water flowing out of the soil (from depths where the soil is unfrozen) due to consolidation.

Where the model has the most layers, especially within a relatively short period of time the model results deviates most from the experimental results. This coincides with the initial deposition and the surface boundary having the most uncertainties, e.g. the settlement behaviour prior to consolidation, the impact of snow and ice cover, cracks, runoff and the impact of using monthly averaged weather data.

DESPOSITION REQUIREMENTS

The ability to numerically simulate the behaviour of atmospheric drying of MFT gives the ability to test various strategies numerically (e.g. Vardon et al., 2015). However, the objective should be clear. The problems of volume reduction, can mostly be solved via flocculation and consolidation processes, with the majority of the reduction in stack height coming from this process, see Figure 5 in combination with Figure 6. Evaporation allows additional reductions of water content, and more limited reductions in void ratios, however it is this final reduction in void ratio which gives significant strength gain. Therefore, timing the layer deposition, so that consolidation processes dominate in times of low evaporation potential and evaporation processes are dominant when there are high evaporation potentials, allows both volume reduction and strength gain to be maximized.

The currently withdrawn directive on how tailings should be disposed of, known as D074 (ERCB, 2009), however, had strength based requirements. A methodology to translate results here into strength-based requirements is proposed. This can

be useful to meet future regulations or can be input into stability or liability calculations.

Locat and Demers (1988) proposed a relationship for the remoulded shear strength (converted to kPa from Pa in the paper):

$$c_u = \left({}^{1.167}/_{LI}\right)^{2.44} \quad (3)$$

where c_u is the remoulded undrained shear strength and *LI* is the liquidity index. *LI* is in turn defined as:

$$LI = \frac{w-LL}{LL-PL} \quad (4)$$

where *w* is the geotechnical water content (mass water / mass solids), *LL* is the Liquid Limit and *PL* is the Plastic Limit. The *LL* and *PL* were determined by Yao et al. (2012) as 66.5 and 22.7 respectively.

Equation (3) and experimentally determined residual strength from the field tests are shown on Figure 8.

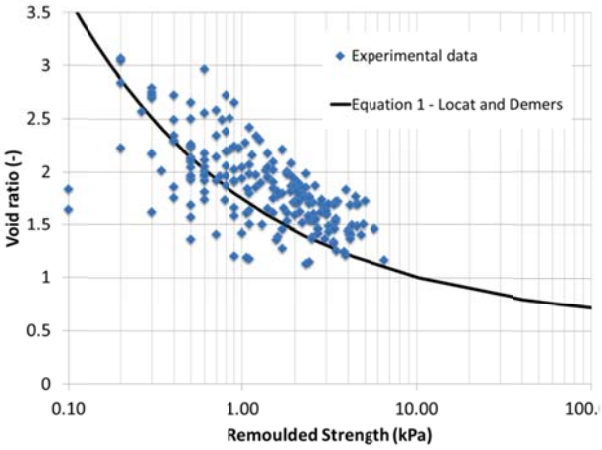

Figure 8. Remoulded undrained shear strength. Blue diamonds are measured data from the Shell field tests (all data aggregated), the solid black line is the proposed relationship from Locat and Demers (1988) (Equation 3).

For the peak strength, the appropriate shear strength for stability analysis, a relationship of the same form, is suggested, with the coefficient and exponent calibrated against experimental evidence, at a reasonable lower bound. The relationship proposed is:

$$c_u = \left({}^{1.5}/_{LI}\right)^{4.0} \quad (5)$$

This relationship, against experimentally determined values is shown in Figure 9.

From this figure, to meet the requirements that were set in D074, a void ratio of below 1.5 would be required. From the results presented, this is only reached at the base of some of the stacks and in the crusts, i.e. the material which has dried significantly due to evaporation.

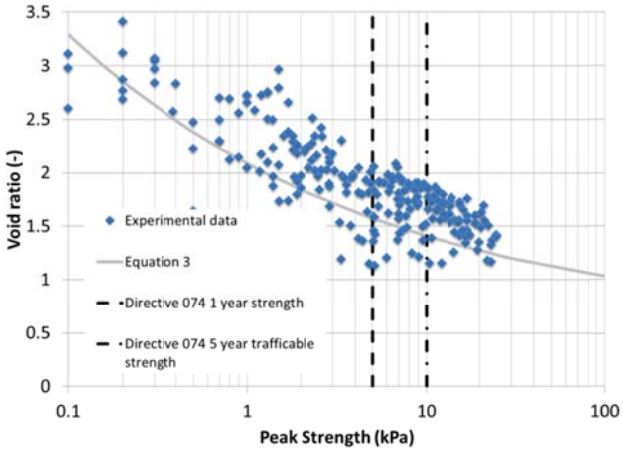

Figure 9. Undrained shear strength. Blue diamonds are measured data from the Shell field tests (all data aggregated) and the grey line is a proposed relationship based upon the experimental data (Equation 5). The vertical lines are the strengths indicated by Directive 074 (ERCB 2009).

To enable the atmospheric drying to achieve maximum volume reduction or maximum strength, evaporative fluxes need to be required to win the boundary condition competition. The requires the consolidation fluxes to be lower than the evaporative fluxes in the periods of time where the potential evaporation is high, i.e. during the summer. The layer size can be tuned so that during the autumn periods, material could be deposited and allowed to consolidate, yielding the majority of the volume reduction and then in the summer allowed to form a crust. Depending on the exact requirements the depth of the layer can

be tuned either based on the consolidation behaviour or the drying behaviour (or a combination).

CONCLUSIONS

The results of the predictive numerical modelling investigation of field tests presented in Vardon et al. (2014) were compared to the experimental results. The model has been shown to be able to predict both qualitatively and quantitatively the behaviour of MFT under AFD field tests.

Initial modelling, based on information received prior to modelling, suggested that more (solid) material was deposited than indicated. Subsequent simulations with additional material yielded improved results, which were able to reproduce almost all features in both a quantitative and qualitative manner. Therefore the model is considered validated in this case.

In addition, a method to predict the strength behaviour based on the void ratio has been initially examined, indicating a method to assess compliance with future regulations or to assess the ongoing changes in stability.

Timing the layer deposition so that consolidation processes dominate first, and volume reduction is maximized, and then afterwards evaporation processes dominate to increase strength (and further reduce volumes) provides an optimal solution. This model allows the numerical investigation of such scenarios to provide optimal solutions which also satisfy regulations.

ACKNOWLEDGMENTS

Funding for this work and field data were provided by Shell Canada. This support is gratefully acknowledged.

REFERENCES

ERCB (2009). Directive 074, Tailings Performance Criteria and Requirements for Oil Sands Mining Schemes, Energy Resources Conservation Board of Alberta.

Locat, J. and Demers, D. (1988). Viscosity, yield stress, remoulded strength, and liquididity index relationships for sensitive clays. Canadian Geotechnical Journal, **25**(4), 799-806.

van der Meulen, J., van Tol, F., van Paassen, L. and Heimovaara, T. (2012). Numerical modeling of drying and consolidation of fine sediments and tailings. IOSTC 2012, 399-409.

Vardon, P.J., Nijssen, T., Yao, Y. and van Tol, A.F. (2014). Numerical simulation of fine oil sand tailings drying in test cells. IOSTC 2014, 59-69.

Vardon, P.J., Yao, Y., van Paassen, L. and van Tol, A.F., (2015). The use of a large-strain consolidation model to optimise multilift tailing deposits. Proceedings of the Tailings and Mine Waste Management for the 21st Century, 263-270, Sydney.

Yao, Y., van Tol, A.F. and van Paassen, L. (2012). The effect of flocculant on the geotechnical properties of mature fine tailings: an experimental study. IOSTC 2012, 391-398.

Yao, Y., van Tol, A.F., van Paassen, L. and Vardon, P.J. (2014). Shrinkage and swelling properties of flocculated mature fine tailings. IOSTC 2014, 27-35.

Yao, Y., van Tol, A.F., van Paassen, L.A. and Vardon, P.J. (2016). Dewatering Behaviour of Fine Oil Sands Tailings: A Summary of Laboratory Results. Submitted to IOSTC 2016.

APPENDIX I

Original numerical predictions against the experimentally recorded results.

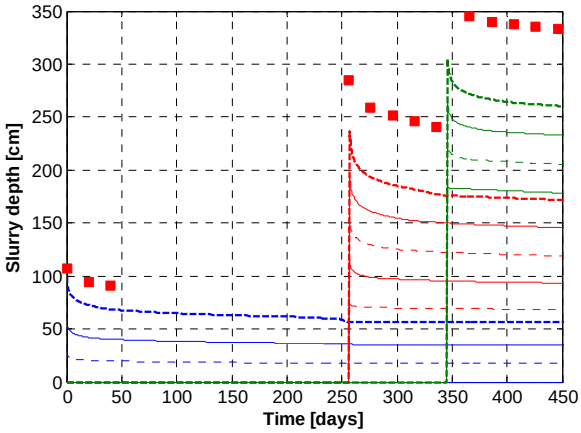

(a) Temporal evolution of the depth. (Numerical results from Figure 17, Vardon et al., 2014).

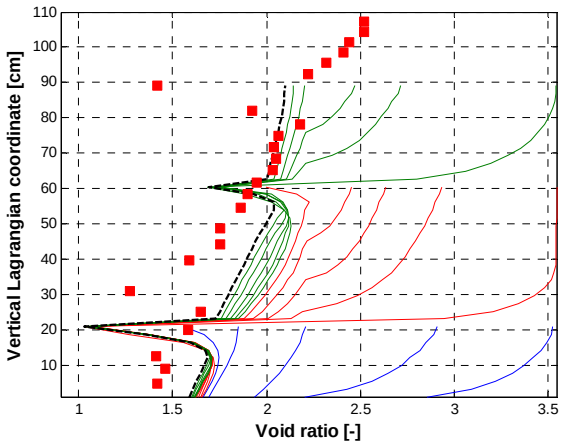

(b) Void ratio profiles in material level (Lagrangian) coordinates with 412 day experimental profile (squares). Final numerical result (thick dotted line) is 450 days. (Numerical results from Figure 19, Vardon et al., 2014)

Figure A1. Comparison of the results of the *Thick Multi-stack* numerical simulation against the experimental results

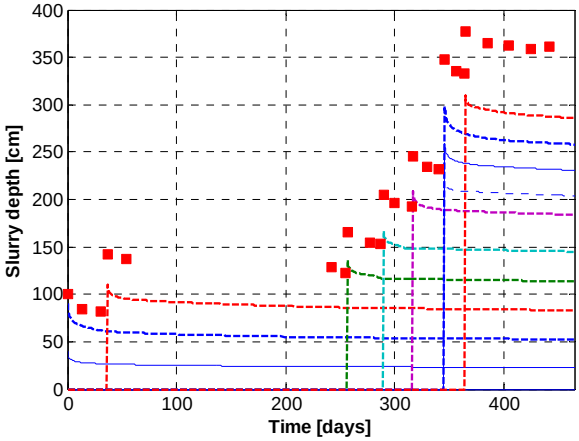

(a) Temporal evolution of the depth.

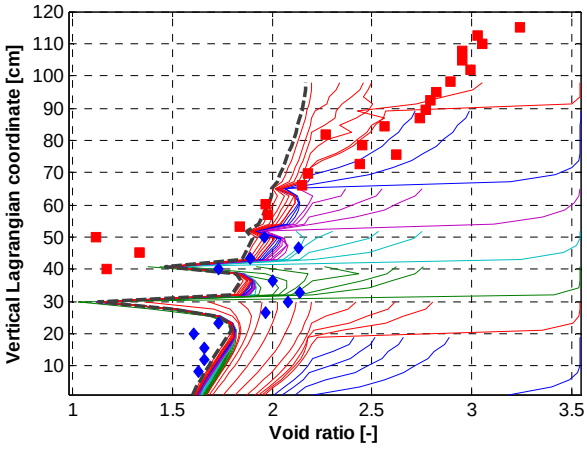

(b) Void ratio profiles in material level (Lagrangian) coordinates with 276 day experimental results (diamonds) and 412 day experimental profile (squares). Final numerical result (thick dotted line) is 450 days. (Numerical results from Figure 21, Vardon et al., 2014).

Figure A2. Comparison of the results of the *Thin Multi-stack* numerical simulation against the experimental results